Int J Adv Manuf Technol (2015) 80:581–590
DOI 10.1007/s00170-015-7034-1

ORIGINAL ARTICLE

Active precision design for complex machine tools: methodology and case study

Yanwei Xu[1,4] · Lianhong Zhang[1] · Shuxin Wang[1] · Hongqi Du[2] · Baolian Chai[2] · S. Jack Hu[3]

Received: 25 September 2014 / Accepted: 13 March 2015 / Published online: 31 March 2015

Abstract Machine tool design starts with the determination of performance specifications. Precision of the NC axes is an important aspect of machine tool design. Conventionally, the precision specification of machine tools is empirically determined, resulting in poor designs with insufficient or excessive precision. To provide a cost-effective precision specification for complex machine tools, such as gear cutting machines, an active precision design approach is proposed to generate the specification of the positioning repeatability of NC axes to meet the designated working precision requirements of the machine tools. The methodology consists of error analysis and precision design in four steps: (1) workpiece surface formation modeling in terms of the motion axes and layout of the machine tool, and the generating principle of workpiece features; (2) workpiece machining error modeling based on the workpiece surface formation model by considering kinematic errors of the NC axes of the machine tool; (3) workpiece machining precision modeling via the machining error model; and (4) precision allocation according to the required workpiece precision and the machining error model. The methodology is demonstrated and validated through a case study of precision design for a six-axis CNC spiral bevel gear milling machine.

Keywords Machine tool · Positioning repeatability · Error analysis · Precision design · Spiral bevel gear · Gear milling machine

1 Introduction

Determination of the performance specifications is the first step in designing a machine tool. Among the performance specifications, precision of NC axes is an important aspect of machine tool design. Insufficient precision will cause an incompetent design, while excessive precision will unnecessarily increase manufacturing cost. Therefore, an appropriate and cost-effective precision specification for machine tools should be determined based on the requirements of workpiece precision or designated working precision requirements of the machine tools.

It has been well understood that the precision of machine tools is affected by several factors, such as the precision of main spindle, slide ways, servo drives, and the stiffness and thermal response of the structure of the machine tools [1, 2]. In the last decades, many researches have been conducted on the precision of machine tools, especially on precision enhancement. Schellekens [3] summarized the rules and principles concerning dimensional metrology, kinematic design, thermal loop, structural loop, metrology frame, drive offset, force compensation, symmetry, and repeatability in design for precision of machine tools.

Error compensation and error elimination have been important methods for enhancing the precision of machine tools

✉ Lianhong Zhang
zhanglh@tju.edu.cn

[1] Key Laboratory of Mechanism Theory and Equipment Design (Tianjin University), Ministry of Education, Tianjin 300072, People's Republic of China

[2] Tianjin No. 1 Machine Tool Works, Tianjin 300180, People's Republic of China

[3] Department of Mechanical Engineering, The University of Michigan, Ann Arbor, MI 48109-2125, USA

[4] School of Mechatronics Engineering, Henan University of Science and Technology, Luoyang 471023, People's Republic of China

[4–13]. Researches on error compensation and error elimination include error identification, measurement, modeling, prediction and compensation, or control [4–6]. Several error compensation methods have been developed, such as computer-aided compensation of geometric and thermal errors [7], shape functions-based interpolation algorithm for error prediction and compensation [8], nonlinear error compensation modeling for geometric and cutting-force induced errors [11], extraction of repeatable errors from random errors and compensation of the repeatable errors by incorporating statistical analysis of measured data [12], and parameterized error modeling and compensation with homogeneous transformation matrices [13].

It has been estimated that thermal deformation weighs about 30–50 % of the overall error of machine tools [14]. However, this can be significantly improved through thermal deformation analysis and control, and thermal error compensation [15–21].

Multi-body system (MBS) theory has also played an effective role in error modeling and compensation of machine tools [14, 22–25]. Zhang et al. [14, 22, 23] and Liu et al. [24] developed general models for geometric errors, load errors and thermal errors, and compensation with MBS kinematics. Fan et al. [25] proposed an MBS-based universal kinematics error modeling and analysis method.

Manufacture of monolithic components and micro-parts has been a hotspot in the recent decades. Precision is also essential to such areas. Researches have been conducted on precision enhancement of machine tools for such applications via fiducials, geometrical analysis, metrology reference transfer, compact and integral design, and using counter motion mechanisms [26–31].

Most up-to-date literatures on precision studies focused on the precision enhancement of machine tools, but limited attention was paid to design of the precision specification of complex machine tools such as the generating-based spiral bevel gear cutting machine. In current practice, precision specification of such machine tools is determined based on the experience of machine tool designers, resulting in a less cost-effective design or poor precision. This paper develops an active precision design approach to determine the precision specification of machine tools. The active precision design is to systematically allocate the machining precision requirement of the workpieces or the designated working precision to the precision specification of the motion axes of the machine in the design phase.

Machine tool precision allocation is similar to but different from tolerance allocation of an assembly. The tolerance allocation assigns the specified assembly tolerance to its components through optimizing manufacturing cost and quality to make the assembly cost-effective [32–35]. They are similar in objective: to make product cost-effective, but different in object and method. The object of the tolerance allocation is the assemblies of a machine, while the object of the precision allocation is the machine. The precision allocation outputs the specified assembly tolerance for the tolerance allocation. On the other hand, there have been lots of methods for the tolerance allocation for assembly, such as proportional scaling, weight factor, least cost optimization, robust tolerance design, etc. [33, 36]. In contrast, the method for the precision allocation of machine tools is still empirical at present. The purpose of this work is to develop an analytic method for the precision allocation of machine tools, especially for precision design of complex machine tools such as gear cutting machines.

The paper is organized as follows: Section 2 presents the methodology of active precision design, Section 3 provides a case study on the repeatability specification design of a six-axis NC spiral bevel gear milling machine, and finally Section 4 concludes the paper.

2 Methodology

The key point of active precision design is to solve the precision specification of machine tools to meet the precision requirement of workpieces or the designated working precision requirements of the machine tools. Since the systematic positional deviation of a NC axis can be compensated, the current work is focused on solving the specification of the positioning repeatability of machine tool NC axes. To simplify the problem definition, the following preliminary assumption is made: the elastic, thermal deformation and geometric errors of machine tools, the installation errors and geometric errors of workpieces, and the systematic positional deviation of NC axes are excluded in the analysis.

A schematic illustration of the methodology is shown in Fig. 1, which consists of two stages: error analysis and precision design. The first stage is a two-step forward analysis, in which the workpiece machining error σ_w versus the position errors σ_i of the NC axes of machine tools is modeled through workpiece surface modeling and subsequent sensitivity K_{mi} analysis of the machining error to the motion errors of the NC axes. In the second stage, workpiece tolerance T_w (i.e., working precision requirement) versus positioning repeatability R_i of NC axes is modeled in light of the concept of process capability C_p and the definition of positioning repeatability. Then the working precision requirement is allocated to the specification of the positioning repeatability of NC axes of machine tools with an equal effects assumption of the positioning repeatability.

2.1 Error analysis

Step 1. Workpiece surface modeling According to the motion axes and layout of a machine tool, the machine coordinate

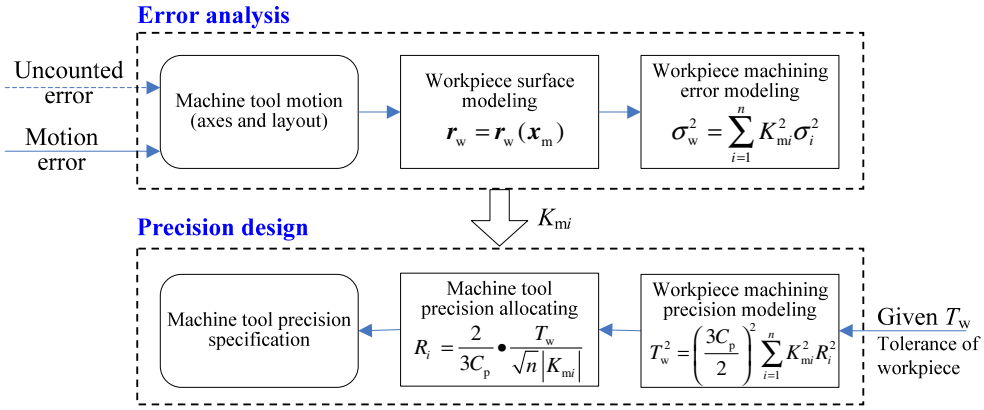

Fig. 1 Schematic illustration of active precision design

frame $\sum_m$ and the workpiece coordinate frame $\sum_w$ can be set up. A point on the cutter in the machine coordinate frame can be transferred to a corresponding point on the workpiece surface in the workpiece coordinate frame in terms of the generating principle of workpiece features. Numerous such corresponding points constitute the surface of the workpiece feature. The surface can be modeled in the workpiece coordinate frame $\sum_w$ as a function of the machine motions.

$$\boldsymbol{r}_w = \boldsymbol{r}_w(x_{m1}, x_{m2}, \ldots, x_{mn}) \tag{1a}$$

where $\boldsymbol{r}_w$ is the position vector of a point on the workpiece surface, x_{mi} (i=1, 2, …, n) is the displacement of NC axis i, and n is the number of NC axes of the machine tool.

Similarly, a specific dimension that scales the machining precision of the workpiece can be consequently expressed as a function of the machine motions.

$$d_w = d_w(x_{m1}, x_{m2}, \ldots, x_{mn}) \tag{1b}$$

Step 2. Workpiece machining error modeling Motion errors Δx_{mi} (i=1, 2, …, n) of the NC axes will cause machining error on the workpiece. The machining error Δd_w of dimension d_w can be approximately expressed as Eq. (2) according to Eq. (1b).

$$\Delta d_w \approx \sum_{i=1}^{n} \frac{\partial d_w}{\partial x_{mi}} \Delta x_{mi} = \sum_{i=1}^{n} K_{mi} \cdot \Delta x_{mi} \tag{2}$$

where, K_{mi} is the sensitivity of the machining error to the motion error of NC axis i, which can be derived through simulating and analyzing the formation of the workpiece surface.

Generally, the motion error Δx_{mi} of the NC axis is independent and follows the normal distribution. According to the principle of error synthesis, the variance of the machining error Δd_w of the workpiece will be

$$\sigma_w^2 = \sum_{i=1}^{n} K_{mi}^2 \sigma_i^2 \tag{3}$$

where σ_i is the standard deviation of the motion error Δx_{mi}.

2.2 Precision design

Step 3. Workpiece machining precision modeling According to the theory of statistical quality control [37], for a given process capability C_p, the machining precision of workpiece, i.e., the tolerance T_w, will be

$$T_w = C_p \times 6\sigma_w \tag{4}$$

In light of ISO 230-2:2006(E) "Test code for machine tools—Part 2: Determination of accuracy and repeatability of positioning numerically controlled axes" [38], the positioning repeatability R_i of NC axis i can be represented as

$$R_i = 4\sigma_i \tag{5}$$

Substitute σ_w in Eq. (4) and σ_i in Eq. (5) into Eq. (3), then the relationship between the machining precision T_w of workpiece and the positioning repeatability R_i (i=1, 2, …, n) of the NC axes will be

$$T_w^2 = \left(\frac{3C_p}{2}\right)^2 \sum_{i=1}^{n} K_{mi}^2 R_i^2 \tag{6}$$

Step 4. Machine tool precision allocation Referring the principle of equal effects of tolerance allocation [39, 40], assume that the positioning repeatability of the NC axes follows the relationship below.

$$K_{mi}^2 R_i^2 = K_{mj}^2 R_j^2 \quad (i, j = 1, 2, \ldots, n;\ i \neq j) \tag{7}$$

Equation (7) means that the repeatability of a NC axis should be inversely proportional to its machining error sensitivity defined in Step 2 and implies that higher precision should be assigned to NC axes of greater machining error sensitivity.

Substitute Eq. (7) into Eq. (6), then the positioning repeatability of NC axis i of the machine tool can be derived as

Eq. (8), which will theoretically meet the machining precision requirement of the workpiece.

$$R_i = \frac{2}{3C_p} \bullet \frac{T_w}{\sqrt{n}|K_{mi}|} \tag{8}$$

Since the elastic and thermal deformation, geometric error of the machine tools, installation error, and geometric error of the workpiece are excluded in the modeling, the current modeling only provide a theoretical reference for the positioning repeatability of the NC axes. A safety factor should be taken to the calculated positioning repeatability from Eq. (8).

3 Case study

This section presents a case study on the application of the active precision design approach to determine the precision specification of a six-axis CNC spiral bevel gear milling machine to demonstrate the methodology. Because of its complexity in motions and structure, an empirically determined precision specification of the spiral bevel gear milling machine may not meet the machining precision requirement of the gear workpieces. Therefore, it is necessary to solve the precision specification accurately with the active precision design approach.

3.1 Generating machining of spiral bevel gears

Spiral bevel gears of circular arc lengthwise tooth curve, as shown in Fig. 2, are generally manufactured through generating machining of face milling by means of the virtual crown gear principle as shown in Figs. 3 and 4 [41–45]. The blade edges of the rotating cutter, whose axis is offset from the axis of the virtual crown gear by a given distance and is fixed on the virtual crown gear, function as a tooth of the virtual crown gear. In machining of a spiral bevel gear, the virtual crown gear and the gear workpiece mesh with each other and rotate around their respective axes with a predetermined ratio of rotation synchronously; as a result, the cutter will gradually cut out a tooth groove in the gear workpiece. When finishing cutting the tooth groove, the virtual crown gear returns to its original position and the gear workpiece rotates to the next indexing position to prepare cutting the next tooth groove. The above procedures repeats until all the teeth are generated.

Fig. 2 Spiral bevel gear set

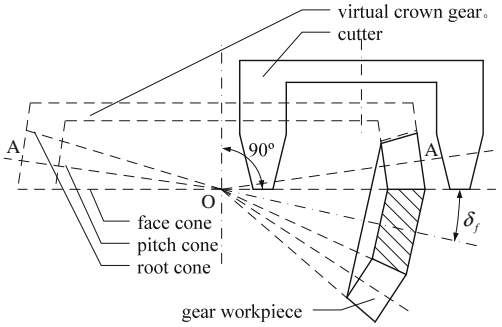

Fig. 3 Cutter, virtual crown gear, and generated gear workpiece

In the case of a Cartesian-type CNC spiral bevel gear milling machine, the rotation of the virtual crown gear is realized through the synchronous translational motions of X and Y axes of the machine, as shown in Fig. 5.

3.2 Cartesian-type CNC spiral bevel gear milling machine

The Cartesian-type CNC spiral bevel gear milling machine was first developed by Gleason Corporation in early 1990s. The CNC machine replaced the conventional cradle mechanism with the synchronous translational NC axes of X and Y to represent the rotation of the virtual crown gear. A schematic illustration of the Cartesian-type CNC spiral bevel gear milling machine is shown in Fig. 5. In addition to X and Y axes, the other axes of the machine are Z for regulating cutting feed, A for rotating the gear workpiece, B for regulating the installation angle of the gear workpiece, and C for rotating the cutter. Axes X, Y, Z, A, and B are driven by servo motors to realize the meshing motion of the virtual crown gear and gear workpiece to cut the tooth grooves of the gear workpiece by generating.

3.3 Modeling of spiral bevel gear tooth surface

Modeling the tooth surface is necessary in order to analyze the machining error of spiral bevel gears. To model the tooth surface, the following coordinate frames are set: the machine coordinate frame $O_mX_mY_mZ_m$ which is marked as $\sum_m$ and is fixed on the machine bed; the gear workpiece coordinate frame $O_wX_wY_wZ_w$ which is marked as $\sum_w$ and is fixed on the gear workpiece, as shown in Fig. 5. The origin O_m of $\sum_m$ is the machine center (the intersection of the axis of the virtual crown gear and the top plane of the cutter); the axes X_m, Y_m, and Z_m of $\sum_m$ parallel the NC axes X, Y, and Z of the

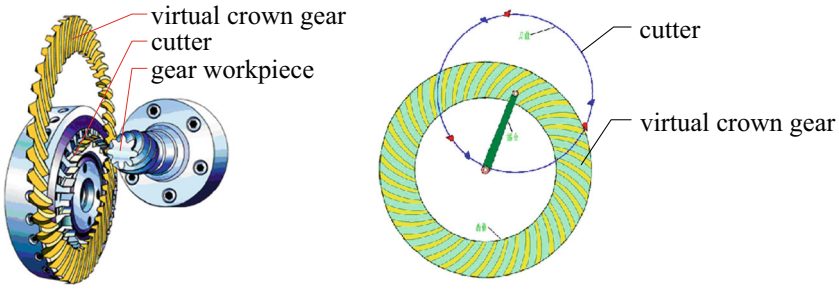

Fig. 4 Schematic illustration of the generating principle of face milling of spiral bevel gear [45]

machine, separately. The origin O_w of $\sum_w$ is the vertex of the design cone of the gear workpiece; the axis X_w of $\sum_w$ coincides with the centerline of the gear workpiece. Figure 6 shows the geometry for modeling the tooth surface of the spiral bevel gear. In Fig. 6, ***i***, ***j***, ***k***, and ***p*** denote unit vectors of the machine coordinate frame.

Tooth surface (generating flank) modeling of the virtual crown gear As shown in Fig. 6 [43], M is a point on the edge and M_0 is a vertex of the edge on the M-O_k section of the cutter, r_{kn} is the radius of the vertices of the cutter edge (subscript n=i denotes the inner edge; subscript n=a denotes the outer edge). The position vector of M_0 is

$$\boldsymbol{r}_{M_0} = \overrightarrow{O_m M_0} = [S_r \cos q + r_{kn} \sin(q-\theta)]\boldsymbol{i} + [S_r \sin q - r_{kn} \cos(q-\theta)]\boldsymbol{j} \quad (9)$$

where S_r and q are the radial and angular position parameters of the cutter center.

$$S_r = \sqrt{X^2 + Y^2},\ q = \arcsin\frac{Y}{S_r} \quad (10)$$

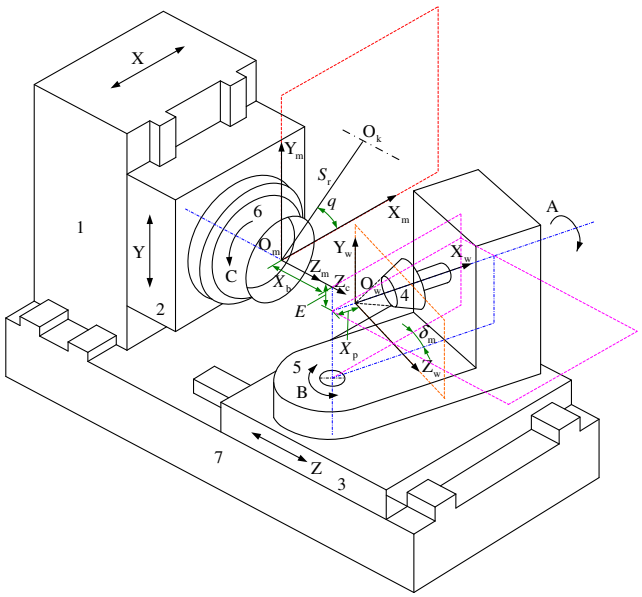

Fig. 5 The Cartesian-type CNC spiral bevel gear milling machine and coordinate frames

The normal vector ***n*** and tangential vector ***t*** of the cutter edge cone at point M is

$$\boldsymbol{n} = \pm\cos\alpha_n \cdot \sin(q-\theta)\boldsymbol{i} \pm \cos\alpha_n \cdot \cos(q-\theta)\boldsymbol{j} - \sin\alpha_n \boldsymbol{k} \quad (11)$$

$$\boldsymbol{t} = \pm\sin\alpha_n \cdot \sin(q-\theta)\boldsymbol{i} \pm \sin\alpha_n \cdot \cos(q-\theta)\boldsymbol{j} + \cos\alpha_n \boldsymbol{k} \quad (12)$$

where θ is the phase angle of point M on the edge cone of the cutter, α_n is the angle between ***n*** and O_kM_0, '±' is '−' when subscript n=i, and '±' is '+' when subscript n=a.

Let $|MM_0| = \mu$, the position vector of point M on the cutter will be

$$\boldsymbol{r}_c = \overrightarrow{O_m M} = \boldsymbol{r}_{M_0} - \mu\boldsymbol{t} \quad (13)$$

Equations (11) and (13) formulate the tooth surface of the virtual crown gear.

Tooth surface modeling of the generated gear When machining a spiral bevel gear by generating, the tooth surface of the generated gear is in conjugation with the tooth surface of the virtual crown gear. If point M is a conjugated contact point on the tooth surfaces of the generated gear and the virtual crown gear, the position vector of point M relative to the origin O_w of the gear workpiece coordinate frame is

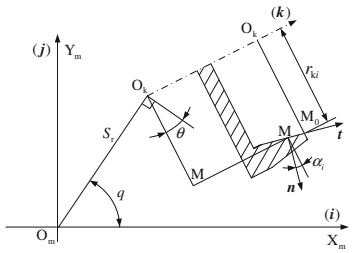

(a) Front view (including half section view of the cutter)

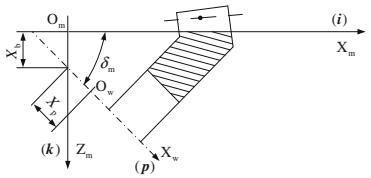

(b) Top view (including half section view of gear workpiece)

Fig. 6 Geometry for tooth surface modeling of spiral bevel gear

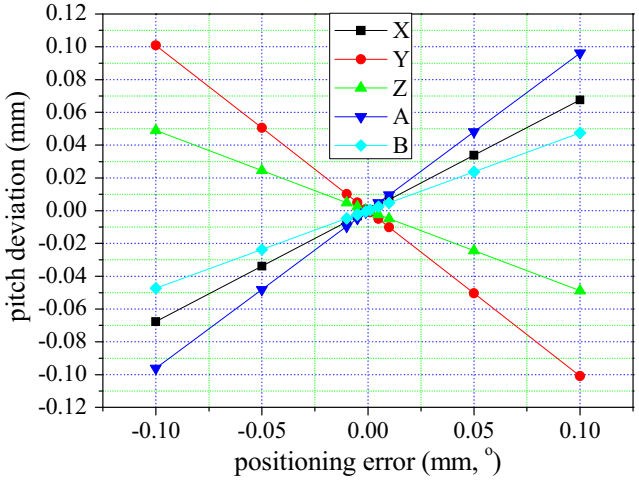

Fig. 7 Relationship of the pitch deviation of a standard tapered spiral bevel gear versus positioning errors of the NC axes of the machine

$$\boldsymbol{r}_2 = \overrightarrow{\mathrm{O_wM}} = \boldsymbol{r}_c + \overrightarrow{\mathrm{O_wO_m}} = \boldsymbol{r}_{M_0} - \mu\boldsymbol{t} + \boldsymbol{m}_2 \tag{14}$$

where

$$\boldsymbol{m}_2 = \overrightarrow{\mathrm{O_wO_m}} = -X_p\boldsymbol{p} - E\boldsymbol{j} - X_b\boldsymbol{k} \tag{15}$$

X_b is the position parameter of the gear workpiece along Z axis, X_p is the position parameter of the gear workpiece along A axis, and E is the offset of the axis of the gear workpiece from that of the virtual crown gear.

In terms of the meshing condition of conjugated surfaces, the relative velocity $v^{(cw)}$ of the virtual crown gear to the gear workpiece and the normal $\boldsymbol{n}$ of the conjugated tooth surfaces at the conjugated contact point M must satisfy

$$\boldsymbol{v}^{(cw)} \cdot \boldsymbol{n} = 0 \tag{16}$$

As shown in Fig. 6, the unit vectors $\boldsymbol{i}$, $\boldsymbol{k}$, and $\boldsymbol{p}$ meet

$$\boldsymbol{p} = \boldsymbol{i}\cos\delta_m + \boldsymbol{k}\sin\delta_m \tag{17}$$

where δ_w is the installation angle of the gear workpiece.

Define i as the ratio of revolution of the gear workpiece to the virtual crown gear and $\boldsymbol{\omega}_c = k$ as the angular velocity of the virtual crown gear, the angular velocity of the gear workpiece will be $\boldsymbol{\omega}_w = i\boldsymbol{p}$, then the relative angular velocity $\boldsymbol{\omega}^{(cw)}$ of the virtual crown gear to the gear workpiece and the relative velocity $\boldsymbol{v}^{(cw)}$ will be

$$\boldsymbol{\omega}^{(cw)} = \boldsymbol{\omega}_c - \boldsymbol{\omega}_w = \boldsymbol{k} - i\boldsymbol{p} \tag{18}$$

$$\begin{aligned}\boldsymbol{v}^{(cw)} &= \boldsymbol{\omega}^{(cw)} \times \boldsymbol{r}_c - \boldsymbol{\omega}_w \times \boldsymbol{m}_2 \\ &= \boldsymbol{\omega}^{(cw)} \times (\boldsymbol{r}_{M_0} - \mu\boldsymbol{t}) - i\boldsymbol{p} \times \boldsymbol{m}_2\end{aligned} \tag{19}$$

Substitute Eq. (19) into Eq. (16), then

$$\left[\boldsymbol{\omega}^{(cw)} \times \boldsymbol{r}_{M_0}\right] \times \boldsymbol{n} - \mu\left[\boldsymbol{\omega}^{(cw)} \times \boldsymbol{t}\right] \times \boldsymbol{n} - i(\boldsymbol{p} \times \boldsymbol{m}_2) \times \boldsymbol{n} = 0 \tag{20}$$

Solving μ from Eq. (18),

$$\mu = \frac{\left[\boldsymbol{\omega}^{(cw)} \times \boldsymbol{r}_{M_0}\right] \times \boldsymbol{n} - i(\boldsymbol{p} \times \boldsymbol{m}_2) \times \boldsymbol{n}}{\left[\boldsymbol{\omega}^{(cw)} \times \boldsymbol{t}\right] \times \boldsymbol{n}} \tag{21}$$

Substituting Eq. (21) into Eq. (14), the position vector of the conjugated contact point of the tooth surface of the generated gear will be determined. Equation (14) formulates the tooth surface of the generated gear.

The above deductions are conducted in the machine coordinate frame $\sum_m$. Equation (14) can be transferred from the machine coordinate frame $\sum_m$ to the gear workpiece coordinate frame $\sum_w$ for convenience.

Similar to Eq. (1a), the tooth surface of the spiral bevel gear defined by Eq. (14) will be a function of the motions of the NC axes of the spiral bevel gear milling machine in the form of Eq. (22).

$$\boldsymbol{r}_2 = \boldsymbol{r}_2(X, Y, Z, A, B) \tag{22}$$

Table 1 Parameters of the benchmark gears (length/mm, angular/°)

No.	Diameter of pitch circle	Number of teeth	Module	Helix angle	Pressure angle	Hand of helix	Pitch cone angle	Root angle	Face width	Addendum	Dedendum
Gear 1	128	32	4	35	20	Right	63.433	59.483	20	2.40	4.96
Gear 2	225	25	9	35	20	Right	66.250	60.580	41	4.78	12.21
Gear 3	248	32	7.75	35	20	Right	63.433	59.183	40	4.32	10.31
Gear 4	320	32	10	35	20	Right	63.433	59.483	50	6	12.4
Gear 5	400	40	10	60	20	Right	63.433	59.483	60	6	12.4
Gear 6	500	50	10	60	20	Right	63.433	61.017	60	6.6	11.8
Gear 7	600	60	10	70	20	Right	63.433	61.450	70	6.8	11.6
Gear 8	700	56	12.5	80	20	Right	63.433	61.333	80	8.625	14.375
Gear 9	750	50	15	90	20	Right	63.433	61.017	90	9.9	17.7

Table 2 Sensitivities of the pitch deviation to the positioning errors

No.	K_{mX} (μm/μm)	K_{mY} (μm/μm)	K_{mZ} (μm/μm)	K_{mA} (μm/″)	K_{mB} (μm/″)
Gear 1	0.6764	−1.0088	−0.4886	0.2669	0.1316
Gear 2	0.5955	−1.0189	−0.4530	0.4544	0.1946
Gear 3	0.6582	−1.0103	−0.4689	0.5144	0.2409
Gear 4	0.6852	−1.0088	−0.4907	0.6673	0.3300
Gear 5	0.6811	−1.0088	−0.4897	0.8395	0.4146
Gear 6	0.7242	−1.0035	−0.4812	1.0819	0.5447
Gear 7	0.6889	−1.0023	−0.4669	1.3027	0.6448
Gear 8	0.7051	−1.0026	−0.4726	1.5234	0.7603
Gear 9	0.7405	−1.0035	−0.4850	1.6229	0.8226

3.4 Modeling of spiral bevel gear machining error

The pitch deviation Δf_{pt} of the spiral bevel gear, i.e., the deviation of the actual pitch from the nominal or theoretical pitch, is selected as the evaluation index of the machining error of the generated gear tooth surface in terms of the China National Standard GB 11365-89 of "Accuracy of Bevel and Hypoid Gears" [46]. The pitch f_{pt} is the arc distance between the two intersection points of the same side surfaces of two adjacent teeth with the pitch circle at the middle of the face width of the spiral bevel gear. The pitch deviation is equivalent to the position error of a specific point on the tooth surface. Similar to Eq. (1b), the pitch f_{pt} will also be a function of the machine motions according to Eq. (22).

$$f_{pt} = f(X, Y, Z, A, B) \tag{23}$$

The pitch deviation Δf_{pt} can be approximately expressed as

$$\begin{aligned}\Delta f_{pt} \approx & \frac{\partial F}{\partial X}\Delta X + \frac{\partial F}{\partial Y}\Delta Y + \frac{\partial F}{\partial Z}\Delta Z + \frac{\partial F}{\partial A}\Delta A + \frac{\partial F}{\partial B}\Delta B \\ = & K_{mX}\Delta X + K_{mY}\Delta Y + K_{mZ}\Delta Z + K_{mA}\Delta A \\ & + K_{mB}\Delta B\end{aligned} \tag{24}$$

Table 3 Limit pitch deviation of the benchmark gears of accuracy grade 6 and the corresponding positioning repeatability of the NC axes (length/μm, angular/″)

No.	Limit pitch deviation	Positioning repeatability				
		X axis	Y axis	Z axis	A axis	B axis
Gear 1	10	5.3	*3.5*	*7.3*	13.4	27.1
Gear 2	16	9.6	5.6	12.6	12.6	29.4
Gear 3	16	8.7	5.7	12.2	11.1	23.7
Gear 4	16	8.3	5.7	11.6	8.6	17.3
Gear 5	16	8.4	5.7	11.7	6.8	13.8
Gear 6	18	8.9	6.4	13.4	5.9	11.8
Gear 7	18	9.3	6.4	13.8	4.9	10.0
Gear 8	20	10.1	7.1	15.1	4.7	9.4
Gear 9	20	9.6	7.1	14.7	*4.4*	*8.7*

The italic data is the minimum of its corresponding column

where, ΔX, ΔY, ΔZ, ΔA, and ΔB are the positioning errors of the NC axes of the machine; K_{mi} (i=X, Y, Z, A, B) is the sensitivity of the pitch deviation to the positioning errors.

As there does not exist an analytic expression of Eq. (23), the pitch deviation can be acquired by means of numerical calculations as follows: By solving the two intersection points of the same side surfaces of two adjacent teeth and the pitch circle at the middle of the face width of the spiral bevel gear, (1) calculate the pitch of the theoretical spiral bevel gear, (2) calculate the pitch of the generated spiral bevel gear with positioning errors of the NC axes, and (3) calculate the pitch deviation. Figure 7 shows typical relationships between the pitch deviation of a generated standard tapered spiral bevel gear and the positioning errors of the NC axes of the spiral bevel gear milling machine. It can be found in Fig. 7 that the pitch deviation varies linearly versus the positioning errors. The sensitivity of the pitch deviation to the positioning errors, K_{mi} (i=X, Y, Z, A, B), are the slopes of the pitch deviation versus positioning error lines in Fig. 7.

According to Eqs. (3) and (24), the standard deviation of machining error of the spiral bevel gear, $\sigma_{f_{pt}}$ is

$$\sigma_{f_{pt}}^2 = K_{mX}^2\sigma_X^2 + K_{mY}^2\sigma_Y^2 + K_{mZ}^2\sigma_Z^2 + K_{mA}^2\sigma_A^2 + K_{mB}^2\sigma_B^2 \tag{25}$$

where σ_i (i=X, Y, Z, A, B) is the standard deviation of the positioning errors of the NC axes of the spiral bevel gear milling machine.

Table 4 Specification of the positioning repeatability of the NC axes of YK2275 milling machine

	X axis	Y axis	Z axis	A axis	B axis
APD[+]	3.5 μm	3.5 μm	7.3 μm	4.4 ″	8.7 ″
EPD[++]	2.0 μm	2.0 μm	2.0 μm	2.0 ″	2.0 ″

[+] *APD* active precision design, [++] *EPD* empirical precision design

3.5 Modeling of spiral bevel gear machining precision

According to Eqs. (4)–(6) and (25), the machining precision of the spiral bevel gear, $T_{wf_{pt}}$ is

$$T^2_{wf_{pt}} = \left(\frac{3C_p}{2}\right)^2 \left(K^2_{mX}R^2_X + K^2_{mY}R^2_Y + K^2_{mZ}R^2_Z + K^2_{mA}R^2_A + K^2_{mB}R^2_B\right) \tag{26}$$

where R_i (i=X, Y, Z, A, B) is the positioning repeatability of axes X, Y, Z, A, and B of the Cartesian-type CNC spiral gear milling machine.

3.6 Allocating of machining precision of spiral bevel gear to positioning precision of NC axes

According to Eqs. (7), (8), and (26), the positioning repeatability of NC axis i of the machine will be derived as

$$R_i = \frac{2}{3C_p}\cdot\frac{T_{wf_{pt}}}{\sqrt{5}|K_{mi}|} = \frac{2}{3C_p}\cdot\frac{2\left|\Delta f_{pt}\right|_{max}}{\sqrt{5}|K_{mi}|} \tag{27}$$

where $\left|\Delta f_{pt}\right|_{max} = T_{wf_{pt}}/2$ is the maximum absolute pitch deviation, which is a specific precision index of a spiral bevel gear of a given accuracy grade.

For a given accuracy grade of a spiral bevel gear, the corresponding positioning repeatability of the NC axes of the machine can be acquired with Eq. (27) when obtained K_{mi} (i=X, Y, Z, A, B) by modeling the machining error of the spiral bevel gears. By calculating and analyzing the positioning repeatability of the NC axes that covers the dimension specification of the gear workpieces of the given accuracy grade, the specification of the positioning repeatability of the NC axes of the Cartesian-type CNC spiral bevel gear milling machine can be resolved.

3.7 Example: precision design of YK2275 CNC spiral bevel gear milling machine

The positioning precision design of a model YK2275 spiral bevel gear milling machine manufactured by Tianjin No. 1 Machine Tool Works is taken as an example to demonstrate the methodology. The machine was designated of a process potential C_p=1.67.

YK2275 is a Cartesian-type CNC spiral bevel gear milling machine as illustrated in Fig. 5. The dimension specification of the gear workpieces of YK2275 is from 100 to 762 mm in pitch circle diameter. The designate machining precision of the gear workpieces is grade 6 of GB11365-89.

Nine benchmark gears of accuracy grade 6 with the pitch circle from 100 to 750 mm covering the dimension specification of the gear workpieces of the machine are selected to resolve the specification of the positioning repeatability of the NC axes of YK2275. The parameters of the gears are shown in Table 1. The sensitivities of the pitch deviation of generated benchmark gears to the positioning errors are shown in Table 2. The limit pitch deviations (the maximum absolute pitch deviations) of the benchmark gears from [46] are shown in Table 3.

Substituting the maximum absolute pitch deviations in Table 3, the corresponding sensitivities in Table 2, and C_p= 1.67 into Eq. (27), the positioning repeatability of the NC axes can be obtained as shown in Table 3. By selecting the minimum of each column of the positioning repeatability of Table 3, the specification of the positioning repeatability of YK2275 is determined as in Table 4. It should be noted that the positioning repeatability specifications of X and Y axes are set to the same value considering their functional equivalency. The positioning repeatability specification by empirical precision design is also listed in Table 4 for comparison. It is significant that the positioning repeatability specification by the active precision design approach is more cost-effective than that by the empirical precision design because of its individualized looser precision.

A mockup of the YK2275 spiral gear milling machine was designed referring the EPD positioning repeatability

Table 5 Test results of positioning repeatability and working precision of YK2275 mockup

Positioning repeatability	X axis	Y axis	Z axis	A axis	B axis	
	2.2 μm	5.9 μm	4.8 μm	3.96″	NA[a]	
Benchmark gear grade 6 of GB11365-89	Number of teeth	Module	Helix angle (right)	Pressure angle	Limit pitch deviation	Measured pitch deviation
	34	7.4 mm	35°	20°	16 μm	15 μm
	K_{mX}	K_{mY}	K_{mZ}	K_{mA}	K_{mB}	
	0.6596 μm/μm	−1.0096 μm/μm	−0.4700 μm/μm	0.5221 μm/″	0.2454 μm/″	

[a] The positioning repeatability of the B axis was not available in the test because of capability limitation of the test instrument

specification in Table 4 and built. Test results of positioning repeatability and working precision of the mockup are presented in Table 5. The working precision test was carried out by machining and measuring a benchmark gear of designated accuracy.

The machining error of the benchmark gear caused by the four NC axes (X, Y, Z and A) can be estimated by substituting into Eq. (26) the sensitivities K_{mi} (i=X, Y, Z and A) and the measured positioning repeatability of the axis in Table 5. The estimated machining error is 12.4 μm, which is about 0.8 or 4/5 times of the measured machining error of the benchmark gear, 15 μm in pitch deviation. This approximately validates Eq. (26), and thus Eq. (27) and the active precision design approach indirectly.

4 Conclusions

An active precision design approach is developed to solve the specification of positioning repeatability of NC axes of machine tools based on the precision requirement of the workpiece.

The approach can be implemented in two stages: (1) error analysis and (2) active precision design. Stage (1) takes motion errors of the machine tools as input and predicts the machining error of the workpiece; while Stage (2) takes machining precision requirement of the workpiece as input and outputs the positioning repeatability specification of the machine tools via the error analysis and the machine tool precision allocating model.

The case study on design of the positioning repeatability specification of NC axes of YK2275 spiral bevel gear milling machine validated the approach. The active design approach is generic and can be applied to all complex machining operations and machine tools. The approach is analytic and modeling-based, which can avoid the inaccuracy of the experience-based precision specification and make the precision specification just-in-need and the machine tools cost-effective. Future studies on the active precision design of machine tools would consider geometric errors, load errors, and thermal errors of the machine tools into the modeling.

Acknowledgments The authors are grateful for the financial support of the National Natural Science Foundation of China under grant No. 50875182 and the National High-tech R&D Program (863 Program) of China under grant No. 2007AA042005.

References

1. Rao SB (1997) Metal cutting machine tool design—a review. J Manuf Sci Eng 119:713–716
2. Hale LC (1999) Principles and techniques for designing precision machines. PhD thesis. Massachusetts Institute of Technology
3. Schellekens P, Rosielle N, Vermeulen H, Vermeulen M, Wetzels S, Pril W (1998) Design for precision: current status and trends. CIRP Ann Manuf Technol 47(2):557–586
4. Ramesh R, Mannan MA, Poo AN (2000) Error compensation in machine tools—a review: part I: geometric, cutting-force induced and fixture-dependent errors. Int J Mach Tools Manuf 40(9):1235–1256
5. Ramesh R, Mannan MA, Poo AN (2000) Error compensation in machine tools—a review: part II: thermal errors. Int J Mach Tools Manuf 40(9):1257–1284
6. Ni J (1997) A perspective review of CNC machine accuracy enhancement through real-time error compensation. Chin Mechanic Eng 8(1):29–33
7. Chen JS (1995) Computer-aided accuracy enhancement for multi-axis CNC machine tool. Int J Mach Tools Manuf 35(4):593–605
8. Wang SM, Liu YL, Kang Y (2002) An efficient error compensation system for CNC multi-axis machines. Int J Mach Tools Manuf 42(11):1235–1245
9. Tsutsumi M, Saito A (2003) Identification and compensation of systematic deviations particular to 5-axis machining centers. Int J Mach Tools Manuf 43(8):771–780
10. Tsutsumi M, Saito A (2004) Identification of angular and positional deviations inherent to 5-axis machining centers with a tilting-rotary table by simultaneous four-axis control movements. Int J Mach Tools Manuf 44(12–13):1333–1342
11. Raksiri C, Parnichkun M (2004) Geometric and force errors compensation in a 3-axis CNC milling machine. Int J Mach Tools Manuf 44(12–13):1283–1291
12. Zhu WD, Wang ZG, Yamazaki K (2010) Machine tool component error extraction and error compensation by incorporating statistical analysis. Int J Mach Tools Manuf 50(9):798–806
13. Jung JH, Choi JP, Lee SJ (2006) Machining accuracy enhancement by compensating for volumetric errors of a machine tool and on-machine measurement. J Mater Process Technol 174(1–3):56–66
14. Zhang Q, Zhao HL, Tang H, Sheng BH (1999) Application of error compensation technique for NC machine tools: thermal error compensation. Manufact Technol Mach Tool 3:26–28
15. Liang RJ, Ye WH, Zhang HY, Yang QF (2012) The thermal error optimization models for CNC machine tools. Int J Adv Manuf Technol 63(9–12):1167–1176
16. Wu CW, Tang CH, Chang CF, Shiao YS (2012) Thermal error compensation method for machine center. Int J Adv Manuf Technol 59(5–8):681–689
17. Guo QJ, Yang JG, Wu H (2010) Application of ACO-BPN to thermal error modeling of NC machine tool. Int J Adv Manuf Technol 50(5–8):667–675
18. Han J, Wang LP, Wang HT, Cheng NB (2012) A new thermal error modeling method for CNC machine tools. Int J Adv Manuf Technol 62(1–4):205–212
19. Tan B, Mao XY, Liu HQ, Li B, He SP, Peng FY, Yin L (2014) A thermal error model for large machine tools that considers environmental thermal hysteresis effects. Int J Mach Tools Manuf 82–83:11–20
20. Li Y, Zhao WH, Wu WW, Lu BH, Chen YB (2014) Thermal error modeling of the spindle based on multiple variables for the precision machine tool. Int J Adv Manuf Technol 72(9–12):1415–1427
21. Huang YQ, Zhang J, Li X, Tian LJ (2014) Thermal error modeling by integrating GA and BP algorithms for the high-speed spindle. Int J Adv Manuf Technol 71(9–12):1669–1675
22. Zhang Q, Wang GF, Liu YW, Zhao HL, Sheng BH (1999) Application of error compensation technique for NC machine tools: geometric error compensation. Manufact Technol Mach Tool 1:30–34
23. Zhang Q, Zhang HG, Liu YW, Zhao HL, Sheng BH, Zhang TC (1999) Application of error compensation technique for NC

machine tools: load error compensation. Manufact Technol Mach Tool 2:8–9
24. Liu YW, Zhang Q, Zhao XS, Zhang ZF, Zhang YD (2002) Multi-body system based technique for compensating thermal errors in machining centers. Chin J Mech Eng 38(1):127–130
25. Fan JW, Guan JL, Wang WC, Luo Q, Zhang XL, Wang LY (2002) A universal modeling method for enhancement the volumetric accuracy of CNC machine tools. J Mater Process Technol 129(1–3):624–628
26. Smith S, Woody BA, Miller JA (2005) Improving the accuracy of large scale monolithic parts using fiducials. CIRP Ann Manuf Technol 54(1):483–486
27. Alberto CR, Leopoldo RH, Tatiana B, Ernst K (2007) Geometrical error analysis of a CNC micro-machine tool. Mechatronics 17(4–5): 231–243
28. Woody BA, Smith KS, Hocken RJ, Miller JA (2007) A technique for enhancing machine tool accuracy by transferring the metrology reference from the machine tool to the workpiece. J Manuf Sci Eng 129(3):636–643
29. Brecher C, Utsch P, Wenzel C (2009) Five-axes accuracy enhancement by compact and integral design. CIRP Ann Manuf Technol 58(1):355–358
30. Wang ZG, Cheng X, Nakamoto K, Kobayashi S, Yamazaki K (2010) Design and development of a precision machine tool using counter motion mechanisms. Int J Machine Tools Manufac 50(4): 357–365
31. Brecher C, Utsch P, Klar R, Wenzel C (2010) Compact design for high precision machine tools. Int J Mach Tools Manuf 50(4):328–334
32. Chase KW, Greenwood WH, Loosli BG, Hauglund LF (1990) Least cost tolerance allocation for mechanical assemblies with automated process selection. Manufac Rev 3(1):49–59
33. Chase KW (1999) Tolerance allocation methods for designers. ADCATS Rep 99(6):1–28
34. Sivakumar K, Balamurugan C, Ramabalan S (2011) Concurrent multi-objective tolerance allocation of mechanical assemblies considering alternative manufacturing process selection. Int J Adv Manuf Technol 53(5–8):711–732
35. Andolfatto L, Thiébaut F, Lartigue C, Douilly M (2014) Quality- and cost-driven assembly technique selection and geometrical tolerance allocation for mechanical structure assembly. J Manuf Syst 33(1):103–115
36. Khodaygan S, Movahhedy MR (2014) Robust tolerance design of mechanical assemblies using a multi-objective optimization formulation. SAE Technical Paper No.2014-01-0378
37. Montgomery DC (2009) Introduction to statistical quality control, 6th edn. Wiley, New York, pp 351–364
38. International Standard ISO 230-2: 2006(E), Test code for machine tools—part 2: determination of accuracy and repeatability of positioning numerically controlled axes
39. Ma H, Wang J (2009) Precision theory of instrument. Press of Beijing University of Aeronautics and Astronautics, Beijing, pp 376–379
40. Jin T (2005) Precision theory and application. Press of University of Science and Technology of China, Hefei, pp 212–214
41. Litivin FL, Fuentes A (2004) Gears geometry and applied theory, 2nd edn. Cambridge University Press, Cambridge, pp 633–644
42. Gonzalez-Perez I, Fuentes A, Hayasaka K (2006) Analytical determination of basic machine-tool settings for generation of spiral bevel gears from blank data. J Mech Des 132(10):101002-1–11
43. Zeng T (1989) Design and machining of spiral bevel gear. Harbin Institute of Technology Press, Harbin, pp 90–91
44. Fan Q (2006) Computerized modeling and simulation of spiral bevel and hypoid gears manufactured by gleason face hobbing process. J Mech Des 128(6):1315–1327
45. Fan Q (2007) Enhanced algorithms of contact simulation for hypoid gear drives produced by face-milling and face-hobbing processes. J Mech Des 129(1):31–37
46. China National Standard GB 11365-89, Accuracy of bevel and hypoid gears